

doi: 10.15407/ujpe61.12.1053

E.F. VENGER,<sup>1</sup> L.YU. MELNICHUK,<sup>2</sup> A.V. MELNICHUK,<sup>2</sup> T.V. SEMIKINA<sup>1</sup><sup>1</sup> V.E. Lashkaryov Institute of Semiconductor Physics, Nat. Acad. of Sci. of Ukraine  
(41, Nauky Ave., Kyiv 03028, Ukraine)<sup>2</sup> Mykola Gogol State University of Nizhyn  
(2, Kropyv'yans'ka Str., Nizhyn 16600, Ukraine; e-mail: mov310@mail.ru)**IR SPECTROSCOPIC STUDY  
OF THIN ZnO FILMS GROWN USING  
THE ATOMIC LAYER DEPOSITION METHOD**PACS 07.57, 68.47 Gh

---

*Using the IR reflection method and the modified method of disturbed total internal reflection (DTIR), thin undoped conducting ZnO films grown with the use of the atomic layer deposition method have been studied theoretically and experimentally for the first time in a spectral interval of 400–1400 cm<sup>-1</sup>. The parameters of ZnO films determined from the IR reflection spectra testify to the presence of frequency “windows” in the DTIR spectra, in which surface phonon and plasmon-phonon polaritons are excited. The theoretical calculations are in good agreement with the experimental results. The dispersion dependences of high- and low-frequency branches of DTIR spectra are plotted and analyzed.*

*Keywords:* disturbed total internal reflection, undoped conducting ZnO films, surface plasmon-phonon polaritons.

**1. Introduction**

The fabrication and research of semiconducting zinc oxide films is one of the most challenging scientific directions in the last decade. Today, the main efforts are aimed at the creation of  $p - n$  junction on the basis of ZnO films for its further application in oxide electronics [1, 2], as well as at the further development of transparent conducting ZnO layers, which are, in addition to other destinations, a construction component for various types of solar cells [1, 3]. Recently, conducting oxide films – in particular, heavily doped ones – have been studied as a promising material for plasmonics [4–8]. This circumstance is related to the fact that metal films or metal particles are applied, as a rule, in plasmonic devices.

However, as was marked in work [6], the plasmon resonance in metals is mainly confined by the resonance wavelength  $\lambda_{\text{res}} < 1 \mu\text{m}$ . Hence, a metal ef-

fectively interacts only with light in the ultra-violet and visible spectral ranges. Moreover, gold and silver, which are widely used in plasmonics, are characterized by substantial energy losses at the plasmon propagation, as the incident wave wavelength increases. Therefore, the creation of materials that would be an alternative to metals is rather a challenging task.

In works [4, 7], it was demonstrated that a resonance with  $\lambda_{\text{res}} \geq 1 \mu\text{m}$  accompanied by the excitation of plasmons in the infra-red (IR) range is observed in heavily doped ZnO films. The authors of work [8] showed that the plasmon resonances with wavelengths from the telecommunication interval (namely, 1.3 and 1.55  $\mu\text{m}$ ) can be obtained in undoped ZnO films as well. Those facts allow ZnO films to be regarded as a promising material for plasmonics and, in particular, telecommunication.

However, in this case, semiconductor films have to satisfy a number of requirements. As a rule, for a semiconducting material to possess metallic proper-

---

© E.F. VENGER, L.YU. MELNICHUK,  
A.V. MELNICHUK, T.V. SEMIKINA, 2016

ties, it has to be heavily doped. However, the doping procedure brings about damages in the crystal lattice and the energy loss growth at the plasmon propagation. Additional requirements to films from the plasmonic viewpoint are a small thickness of the films (not exceeding 300 nm) and a small roughness of their surface [6]. Zinc oxide films fabricated with the use of the method of atomic layer deposition (ALD) satisfy those requirements quite well. A detailed description of the method can be found in work [9]. Its unique feature consists in the opportunity to deposit polycrystalline films with a high quality of the crystal lattice, even if the layer thickness amounts to 0.2  $\mu\text{m}$  [10]. The method also allows a high concentration of free charge carriers in a film,  $n_0 = 10^{20} \text{ cm}^{-3}$ , to be achieved without film doping [2].

However, despite a considerable body of publications on zinc oxide films, the literature data are scarce concerning the study of the interaction between the electromagnetic radiation and oscillations of various types, e.g. phonons and plasmons, as well as the conditions, under which the surface polaritons are excited and propagate in thin transparent polycrystalline undoped ZnO films deposited on optical glass substrates. Therefore, in this work, the structures of ZnO films created on the optical glass and silicon substrates with the help of the ALD technique are studied by the methods of infra-red and polariton spectroscopy. Theoretical and experimental researches are carried out for those regions in thin transparent polycrystalline films of undoped zinc oxide deposited on optical glass substrates, where the existence, excitation, and propagation of surface polaritons are possible. The researches were performed for various concentrations of free charge carriers (electrons) in the films and various film thicknesses.

## **2. Thin Film Fabrication and Experimental Technique**

Zinc oxide films were deposited onto silicon and optical glass substrates. Both the glass and silicon substrates were simultaneously treated in a reaction chamber of the technological equipment, a Cambridge NanoTech Savannah-100 ALD reactor. The structures obtained on silicon substrates were used for optical measurements in the reflection geometry. Optical glass was chosen to study surface polaritons of the phonon and plasmon-phonon types be-

cause of the absence of oscillations in the infra-red spectral interval in this material.

The films were grown with the use of diethyl zinc and deionized water vapors as precursors of zinc and oxygen, respectively. Two batches of specimens were fabricated. The first one included specimens III-1 and III-2, and the second one specimens 312-1, 312-2, and 312-3. Specimens in each of the batches had different thicknesses, which was ensured by applying different numbers of treatment cycles at the fabrication.

The inflow time for the reaction gases and nitrogen (to clean the chamber) were identical for the specimens in the same batch. The batches differed from one another in the inflow time of precursors and nitrogen. The change of the gas inflow time gave rise to structural variations at the film growth. In this work, to present the results of our research, we selected two batches of specimens, for which the crystal structures of the films were almost identical. A detailed study of the structural properties of the films and the influence of various technological factors on them can be found in works [2, 3, 10–12].

The deposition temperature was selected to equal 200  $^{\circ}\text{C}$ , because this is the temperature, at which the crystal lattice parameters  $c$  and  $a$  (the  $c$ -axis was directed perpendicularly to the film surface) coincided with the corresponding parameters in the bulk ZnO single crystal. The time of the reaction gas inflow was chosen to produce films with the highest conductivity that can be obtained for undoped specimens (it corresponded to a free charge carrier concentration of  $10^{20} \text{ cm}^{-3}$ ). The film conductivity and the concentration and mobility of free charges were determined from the Hall effect measurements, which were carried out at room temperature on the equipment RH 2035 Phys Tech GmbH after depositing the metal contacts Ti(100  $\text{\AA}$ )/Au (400  $\text{\AA}$ ) on the structure.

In order to fabricate films with various thicknesses, the number of deposition cycles was varied. The thickness of films deposited onto silicon was measured on a spectroscopic reflectometer Micropack Nanocalc 2000. The measurements on an atomic force microscope (Veeco Digital Instruments) showed that the film surface was atomically flat with a maximum root-mean-square roughness of 4 nm.

The spectra of IR reflection and disturbed total internal reflection were measured at room temperature on a spectrophotometer IKS-31 equipped with reflection attachments IPO-22 and NOVO-2, by us-

ing a reference mirror in a frequency interval of 400–1400  $\text{cm}^{-1}$ . The  $R(\nu)$  and  $I(\nu)/I_0(\nu)$  spectra were recorded with the use of a polarizer with the polarization degree  $P = 0.98$ . The reflection coefficient  $R(\nu)$  and the DTIR coefficient were determined with an error of 2–3%. The spectra were measured at the temperature  $T = 300$  K.

### 3. Theory and Analysis of IR Reflection Spectra

A detailed analysis of the procedure aimed at obtaining the mutually consistent parameters in the one-oscillator model for ZnO was performed in works [13, 14]. The authors of work [14] showed that ZnO is characterized by a considerable anisotropy of properties for the phonon subsystem and a weak anisotropy of the plasma subsystem. Owing to this fact, zinc oxide films are good model objects, which are convenient for the research of the anisotropies of optical and electrophysical properties in the IR spectral region, where long-wave optical vibrations of the lattice are coupled with the electron plasma.

The region of “residual rays” for zinc oxide is located between the frequencies of transverse and longitudinal optical phonons (Table 1). Taking into account that ZnO films are polycrystalline, we took the parameters quoted in Table 1 for the one-oscillator model of ZnO single crystals at the orientation  $E \perp C$ . The theoretical calculations of IR reflection spectra for the absorbing film on a “semiinfinite” optical-glass substrate in the frequency interval of “residual rays” for zinc oxide were fulfilled according to mathematical expressions of work [13].

The dependences  $R(\nu)$  and  $I(\nu)/I_0(\nu)$  were calculated on the basis of a model for the dielectric permittivity with additive contributions of active optical phonons and plasmons [15, 16]:

$$\begin{aligned} \varepsilon_j(\nu) = & \varepsilon_{1j}(\nu) + i\varepsilon_{2j}(\nu) = \varepsilon_{\infty j} + \\ & + [\varepsilon_{\infty j}(\nu_{Lj}^2 - \nu_{Tj}^2)] / [\nu_{Tj}^2 - \nu^2 - i\nu\gamma_{fj}] - \\ & - (\nu_{pj}^2 \varepsilon_{\infty j}) / [\nu(\nu + i\gamma_{pj})], \end{aligned}$$

where  $\nu_L$  and  $\nu_T$  are the frequencies of transverse and longitudinal, respectively, optical phonons;  $\gamma_f$  is the damping coefficient of optical phonons;  $\gamma_p$  and  $\nu_p$  are the damping coefficient and the frequency, respectively, of the plasma resonance;  $E$  is the electric vector of infra-red radiation; and  $\nu$  the frequency of

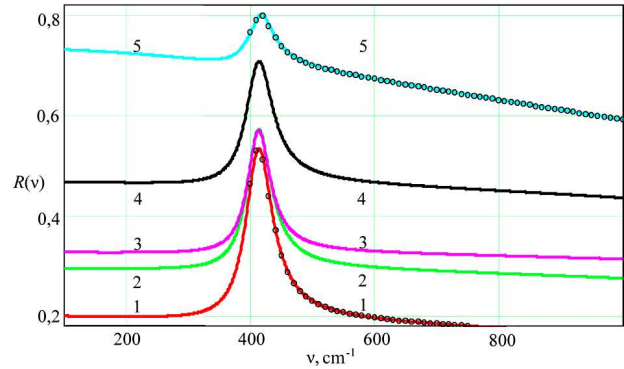


**Fig. 1.** Theoretical spectra  $R(\nu)$  for doped ZnO films on Si substrates (curves) and experimental data (symbols). The calculation parameters are quoted in Table 1

IR radiation (in inverse centimeters). The researches were carried out making no allowance for the substrate absorption in the IR spectral interval.

In Fig. 1, the frequency dependences of the external IR reflection coefficient from the ZnO/Si structure calculated for the film parameters quoted in Table 2 and at the orientation  $E \perp C$  are depicted by curves. Curves 1 and 2 correspond to the film thickness  $d_f = 0.22 \mu\text{m}$  and free charge carrier concentrations of  $1.5 \times 10^{20}$  and  $7.35 \times 10^{19} \text{cm}^{-3}$ , respectively. Curves 3 to 5 were calculated for the film thickness varied from 0.22 to  $0.72 \mu\text{m}$  and the free charge carrier concentration from  $1.3 \times 10^{20}$  to  $4.3 \times 10^{20} \text{cm}^{-3}$ . As one can see, the change of the film thickness and the concentration of free charge carriers (electrons) gives rise to an increase of the reflection coefficient  $R(\nu)$  in the interval of “residual rays” for zinc oxide. The symbols in the plot correspond to the experimental data for the spectra of IR reflection from the ZnO/Si structure (the data for specimens S312-1 and S312-3 are given in Table 2). The step of scanning over the frequency amounted to  $5 \text{cm}^{-1}$ .

The growth of the electron concentration in the zinc oxide films from  $10^{19}$  to  $5 \times 10^{20} \text{cm}^{-3}$  results in the shift of the reflection spectrum maxi-

**Table 1. Mutually consistent parameters of the one-oscillator model for ZnO single crystals [13, 14]**

Orientation	$\varepsilon_0$	$\varepsilon_\infty$	$\nu_T, \text{cm}^{-1}$	$\nu_L, \text{cm}^{-1}$
$E \perp C$	8.1	3.95	412	591
$E \parallel C$	9.0	4.05	380	570

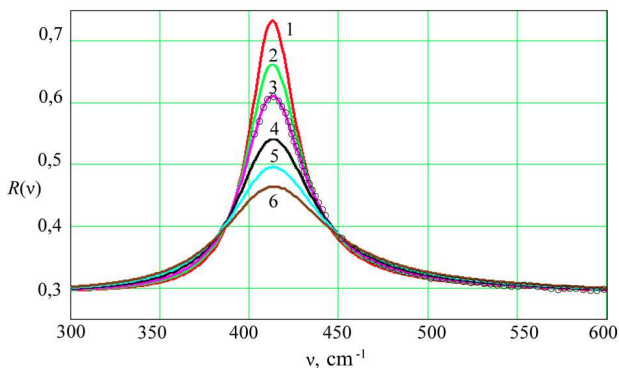


**Fig. 2.** Theoretical spectra  $R(\nu)$  of a doped ZnO film (the film thickness  $d_f = 0.22 \mu\text{m}$ ) on the  $\text{SiO}_2$  substrate ( $\nu_p = \gamma_p = 2530 \text{ cm}^{-1}$ ) for  $\gamma_f = 10, 15, 20, 30, 40,$  and  $50 \text{ cm}^{-1}$  (curves) and experimental data (symbols)

mum in the frequency interval of transverse optical phonons by  $10 \text{ cm}^{-1}$ . The corresponding reflection coefficient increases at that from 0.2 (curve 1) to 0.71 (curve 5) in the whole spectral interval. The calculation was carried out, by using the data for the film thickness and the concentration of free charge carriers obtained from the measurements on a spectroscopic reflectometer and from the Hall effect (see Table 2). Curves 1 to 5 were calculated, by assuming that the condition  $\nu_p = \gamma_p$  for the plasmon damping coefficients is satisfied. While calculating the reflection spectra, the mutually consistent parameters of zinc oxide (see Table 1) were used. The damping of the phonon subsystem was taken to equal  $25 \text{ cm}^{-1}$  for every specimen. The indicated parameters provide the best agreement between the theory and the experimental data. The corresponding error does not exceed 3%.

In Fig. 2, the theoretical and experimental IR reflection spectra for the ZnO/Si structure (specimen S312-2 on silicon) are shown. For all curves, the electron concentration in the ZnO film  $n_0 = 7.35 \times 10^{19} \text{ cm}^{-3}$  and the film thickness  $d_f = 0.22 \mu\text{m}$ . The plasmon damping  $\gamma_p = 2530 \text{ cm}^{-1}$  was also fixed for all specimens. The shape modification of the indicated curves is associated with the influence of the phonon subsystem on the reflection coefficient in the interval of residual rays. Figure 2 testifies to an excellent agreement between the theory and the experiment.

A characteristic feature of all spectra in Figs. 1 and 2 is the presence of maxima in an interval of

$350\text{--}500 \text{ cm}^{-1}$ . They result from the influence of the phonon and plasma subsystems in the interval of “residual rays” of zinc oxide. The reduction of  $R(\nu)$  in an interval of  $300\text{--}600 \text{ cm}^{-1}$  is connected with the influence of not only the concentration, but also the mobility of electrons on the shape of the reflection spectrum. From Fig. 2, one can see that the interval between the frequencies of the transverse and longitudinal optical phonons in a ZnO film is the most sensitive to variations of the concentration and the mobility of free charge carriers in the ZnO/Si structure. However, changes in the plasma subsystem practically do not affect the reflection spectrum of optical glass. The reflection coefficient in an interval of  $300\text{--}600 \text{ cm}^{-1}$  is the most sensitive to the variation of the film thickness.

#### 4. Calculation and Analysis of DTIR Spectra

The data obtained above allowed us to comprehensively research ZnO films on “semiinfinite” optical glass substrates in the case  $E \perp C$ , by using the polariton spectroscopy method. The essence of the DTIR method is as follows [13, 17]. Under the condition of total internal reflection, a ray of IR radiation can penetrate from an optically denser medium, which is transparent in the IR spectral interval, into an optically less dense medium to a depth that is comparable with the wavelength of an incident IR wave. In this case, if the optically less dense medium absorbs, the intensity of light that penetrates into the examined medium becomes weakened, so that the reflection is not total. One should bear in mind that the examined medium strongly absorbs in the IR interval. As a result, the spectral devices will register spectra of the disturbed total internal reflection.

The DTIR spectra were calculated, by using the mathematical expressions obtained in work [13], which involve the interaction of IR radiation with the phonon and plasma subsystems of the ZnO film deposited on a “semiinfinite” optical glass substrate in the case  $E \perp C$ . The mutually consistent parameters for zinc oxide quoted in Table 1 were used in calculations. In addition, all calculations were carried out, by assuming the condition  $\nu_p = \gamma_p$  for the damping coefficients of plasmons in ZnO films. The damping in the phonon subsystem was also taken identical ( $15 \text{ cm}^{-1}$ ) for all specimens. As was shown in works

Table 2. Parameters of doped ZnO films

No.	Specimen	Film thickness, nm	Electron concentration, $\text{cm}^{-3}$	Plasma frequency, $\text{cm}^{-1}$	Mobility, $\text{cm}^2/\text{V}/\text{s}$	Conductivity, $\Omega^{-1}\text{cm}^{-1}$
1	ZnO (S312-1)	220	$1.5 \times 10^{20}$	1140	24	$1.73 \times 10^3$
2	ZnO (S312-1)	220	$7.35 \times 10^{19}$	2530	23.3	$3.65 \times 10^2$
3	ZnO(III-2)	203.2	$1.3 \times 10^{20}$	3370	24.8	$1.94 \times 10^3$
4	ZnI(III-1)	380.8	$1.42 \times 10^{20}$	3520	26.5	$1.66 \times 10^3$
5	ZnOS312-3	720	$4.33 \times 10^{20}$	6145	25.7	$5.6 \times 10^3$

[18, 19], the indicated parameters provided the best agreement of the theory with experimental data (Table 2). The corresponding error did not exceed 3%.

In Fig. 3, the calculated frequency dependences of the DTIR coefficient for ZnO films deposited onto optically isotropic substrates made of optical glass are depicted. The film parameters used in calculations are shown in Tables 1 and 2. The orientation  $E \perp C$  was considered. The film thickness was taken  $d_f = 0.22 \mu\text{m}$ . The concentration of free charge carriers (electrons) amounted to  $1.5 \times 10^{20}$  (curves 1),  $7.35 \times 10^{19}$  (curves 2), and  $1.3 \times 10^{20} \text{ cm}^{-3}$  (curves 3). The theoretical calculations were carried out under the assumption that the value of damping coefficient for the phonon subsystem  $\gamma_f = 15 \text{ cm}^{-1}$ , the gap thickness in the DTIR prism  $d_g = 5 \mu\text{m}$ , and the incidence angle of IR radiation in a DTIR prism  $\varphi = 40^\circ$ .

As one can see from Fig. 3, *a*, a change of the electron concentration in the zinc oxide film with fixed thickness and phonon damping coefficient gives rise to a growth of the DTIR spectrum “half-width”. This tendency is observed for all specimens. In particular, the spectral “half-width” increases from  $33 \text{ cm}^{-1}$  for curve 1 to  $75 \text{ cm}^{-1}$  for curve 3. According to the data of work [13], this fact testifies to an increase of the damping coefficient for surface polaritons in a zinc oxide film, when the degree of film doping grows. A similar tendency is also observed for the curves exhibited in Figs. 3, *b* and *c*, which were calculated, by using the parameters indicated above, but for  $\gamma_f = 30 \text{ cm}^{-1}$  (panel *b*) and  $45 \text{ cm}^{-1}$  (panel *c*). Curves 1 in Fig. 3 well illustrate the increase of the DTIR spectrum “half-width” from 33 to  $69 \text{ cm}^{-1}$ , when the damping coefficient of the phonon subsystem changes from 15 to  $45 \text{ cm}^{-1}$ .

The following facts testify to the excitation of surface polaritons in the ZnO-optical glass system. The

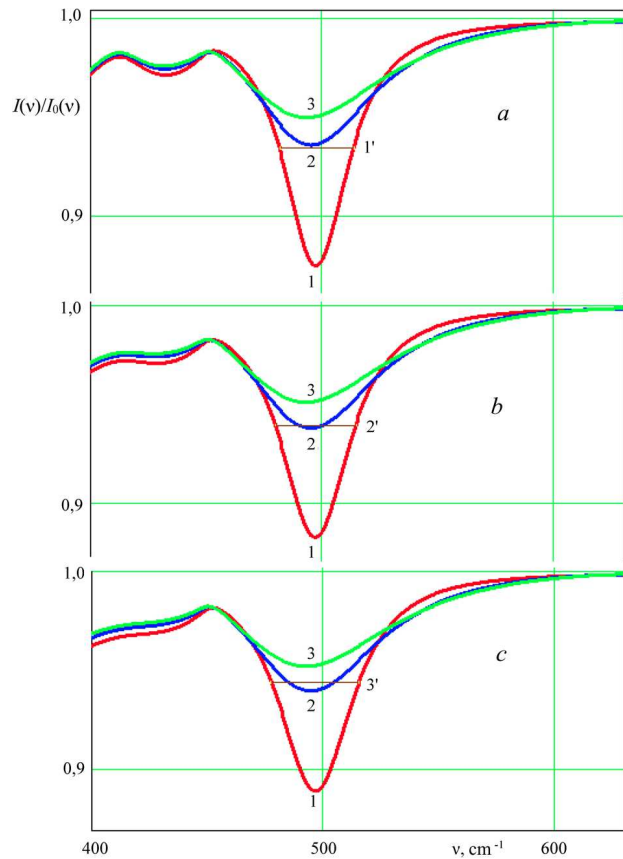
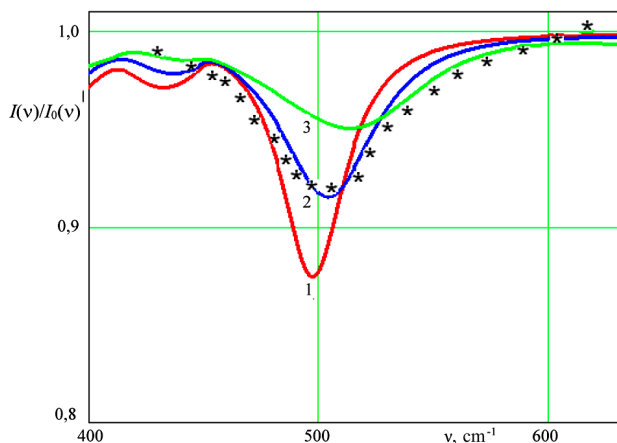
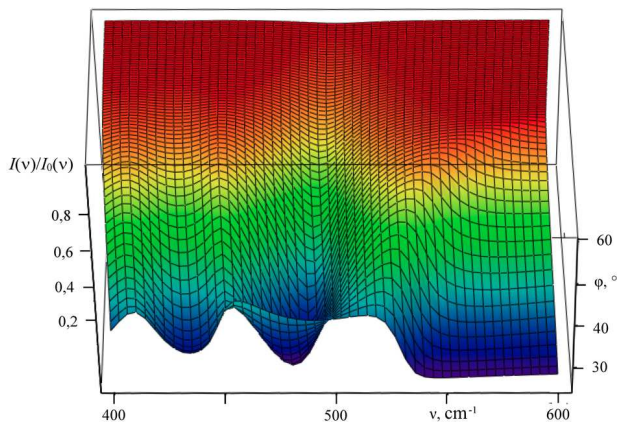


Fig. 3. Theoretical DTIR spectra of a doped ZnO film on the optical glass substrate in the interval of “residual rays” of zinc oxide

minima in the DTIR spectra are observed only in the case of *p*-polarized IR radiation. Those minima are located in the spectral interval, where the dielectric permittivity is negative, i.e. between the frequencies of the transverse and longitudinal optical phonons. Moreover, the minimum in the DTIR spectrum shifts toward high frequencies, when the angle of



**Fig. 4.** DTIR spectra of the structure ZnO-optical glass calculated for  $d_f = 0.22$  (curve 1),  $0.38$  (curve 2), and  $0.72 \mu\text{m}$  (curve 3), and experimental data for  $d_f = 0.38 \mu\text{m}$  (symbols)



**Fig. 5.** Two-dimensional DTIR spectrum calculated for a ZnO film on the optical glass substrate in the geometry  $E \perp C$

light incidence in the DTIR prism increases, and when the absorption intensity decreases, provided that the gap between a DTIR prism and the ZnO-optical glass system remains invariant [13, 17].

Figure 4 demonstrates the DTIR spectra calculated for the ZnO-optical glass structure with various film thicknesses varied from  $0.22$  to  $0.72 \mu\text{m}$ . The theoretical spectra (curves) were obtained for the angle of light incidence in the DTIR element  $\varphi = 40^\circ$ . The DTIR spectra reveal the minima at frequencies of  $496$  (curve 1),  $504$  (curve 2), and  $513 \text{ cm}^{-1}$  (curve 3). As one can see, the increase of the film thickness is accompanied by a shift of the surface polariton frequency toward higher values and a growth of the po-

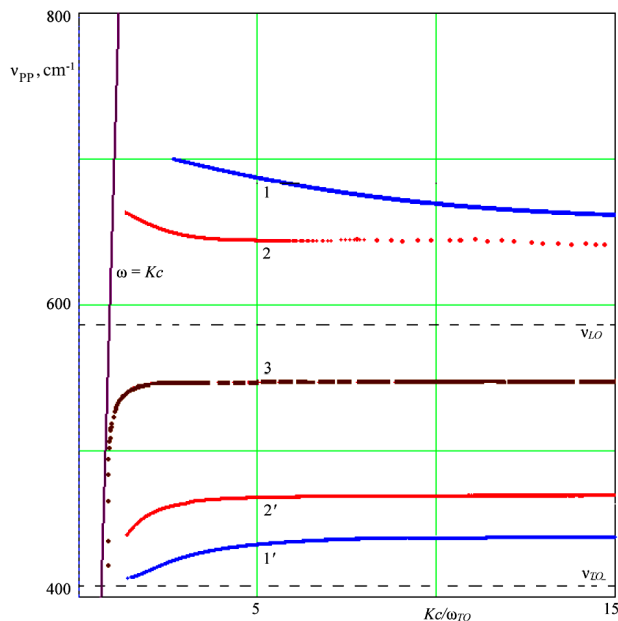


**Fig. 6.** Surface polariton dispersion branches for a ZnO film on the optical glass substrate calculated for  $E \perp C$  and various  $d_f$ -values

lariton peak “half-width”, which is associated with the influence of the phonon subsystem in the zinc oxide film on the surface polariton spectrum in the interval of zinc oxide “residual rays”.

The symbols in Fig. 4 illustrate the experimental DTIR spectrum registered for the ZnO-optical glass system in the case where a doped semiconductor film was deposited onto a “semiinfinite” dielectric substrate with the orientations  $K \perp C$  and  $xy \parallel C$ . The data are presented for specimen S312-2 (the ZnO film on the silicon substrate). The film thickness  $d_f = 0.38 \mu\text{m}$ . The spectrum was recorded at the air gap  $d_g = 5 \mu\text{m}$  between the DTIR element in the KRS-5 and the specimen, and the angle  $\varphi = 40^\circ$  in the DTIR element. The frequency scanning step was equal to  $5 \text{ cm}^{-1}$ . The DTIR spectrum reveals a minimum at a frequency of  $508 \text{ cm}^{-1}$ , which agrees with a calculated result of  $504 \text{ cm}^{-1}$  (see curve 2) within the calculation error limits.

It is evident that the most precise data can be obtained, while plotting the so-called DTIR surface,  $I(\nu)/I_0(\nu)$ , which is a three-dimensional representation of the transmittance of the system concerned and depends on both the radiation frequency and the incidence angle. In the absence of the interaction be-

tween radiation and the structure surface, we have  $I(\nu)/I_0(\nu) = 1$ , so that the DTIR surface is flat in this region. However, in the case where surface polaritons are excited in the ZnO film or in the substrate made of optical glass, the DTIR surface demonstrates a number of “gorges” (Fig. 5). The depth of the latter depends on the following parameters: the gap width  $d_g$  between the DTIR semicylinder and the specimen, radiation frequency  $\nu$ , and so forth. The presence of surface polaritons in the zinc oxide–optical glass system is confirmed by the fact that, as the incident angle increases, the frequency of the minimum in the DTIR spectra shifts toward low frequencies (see Fig. 4), and the spectral “half-width” diminishes.

From the results of our theoretical calculations and the analysis of the data in work [13], we may draw conclusion that the dispersion character of the polariton branches does not change qualitatively, when the thickness of a zinc oxide film is varied. However, quantitative changes are observed. In our opinion, they are caused by a growth of the effective part of the dielectric permittivity in the IR spectral interval.

In Fig. 6, the high- (curves 1 and 2) and low-frequency (curves 1' and 2') dispersion branches for surface polaritons in doped ZnO films 0.22 and 0.72  $\mu\text{m}$ , respectively, in thickness are shown. The dispersion manifests itself in the frequency interval of “residual rays” of ZnO films (412–591  $\text{cm}^{-1}$ ) on the optical glass substrate. This is a frequency interval, where the real part of the dielectric permittivity of a ZnO film is negative, and the energy losses are infinitesimally low. The dispersion branches in the ZnO–optical glass system were calculated, by using the formulas that did not make allowance for the anisotropy of oscillations in the film [19, 20]. One can see that two branches are observed in this system at  $d_f \leq 0.72 \mu\text{m}$ . Similar data were obtained earlier in work [20] for the system ZnO/Al<sub>2</sub>O<sub>3</sub>. The solution of the corresponding equations is the low- (curves 1' and 2') and high-frequency (curves 1 and 2) dispersion branches.

From the analysis of DTIR spectra and dispersion branches (Fig. 6) plotted for various film thicknesses, it follows that a decrease of the film thickness makes the distance between the minima in the DTIR spectra shorter and, consequently, the dispersion branches closer to one another. As is seen from the dispersion curves, the high-frequency branch for the zinc oxide films ( $n_0 = 1.5 \times 10^{20} \text{ cm}^{-3}$ ) with  $d_f \leq 0.22 \mu\text{m}$

is located above the frequency of longitudinal optical phonons in zinc oxide. Our calculations show that, if the thickness of a ZnO film grows, the both branches approach each other. For the film thickness  $d_f \geq 0.5 \mu\text{m}$ , the curves practically coincide (Fig. 6, curve 3), which correlates with the data of work [13] for a ZnO single crystal.

## 5. Conclusions

In this work, the undoped conducting films of zinc oxide deposited with the use of the atomic layer deposition method onto silicon and optical glass substrates have been studied for the first time by applying the methods of IR spectroscopy and disturbed total internal reflection. From the results of combined researches, it follows that the IR reflection and DTIR spectra for the structure air – ZnO film – optical glass are well approximated, by using a mutually consistent set of bulk parameters for single-crystalline zinc oxide obtained in works [2, 14]. The presence of frequency “windows” for the excitation and propagation of surface phonon and plasmon-phonon polaritons is demonstrated. Three-dimensional DTIR spectra (the simultaneous scanning over the incidence angle and the IR radiation frequency) for the structure concerned are plotted for the first time. The dispersion dependences for the high- and low-frequency branches are obtained.

*T.V.S. expresses her gratitude to Marek Godlewski (Institute of Physics, Polish Academy of Sciences, Warsaw, Poland) for the opportunity to use technological and experimental facilities.*

1. T.V. Semikina, V.N. Komashchenko, L.N. Shmyryeva. Oxide electronics as one of transparent electronics directions. *Elektron. Svyaz Elektron. Nanotekhnol.* **3**, 20 (2010) (in Russian).
2. S. Gieraltowska, L. Wachinski, B.S. Witkowski, M. Godlewski, E. Guziewicz. Atomic layer deposition grown composite dielectric oxides and ZnO for transparent electronic applications. *Thin Solid Films* **520**, 4694 (2012) [DOI: 10.1016/j.tsf.2011.10.151].
3. T.V. Semikina, S.V. Mamykin, M. Godlewski, G. Luka, R. Pietruszka, K. Kopalko, T.A. Krajewski, S. Gieraltowska, L. Wachnicki, and L.N. Shmyryeva. ZnO as a conductive layer prepared by ALD for solar cells based on n-CdS/n-CdTe/p-Cu<sub>1.8</sub>S heterostructure. *Semicond. Phys. Quant. Electron. Optoelectron.* **16** (2), 111 (2013) [DOI: 10.15407/spqeo16.02.111].

4. S. Sadofev, S. Kalusniak, P. Schofer, and F. Henneberger. Molecular beam epitaxy of n-Zn(Mg)O as a low-damping plasmonic material at telecommunication wavelengths. *Appl. Phys. Lett.* **102**, 181905 (2013) [DOI: 10.1063/1.4804366].
5. G.V. Naik, J. Kim, and A. Boltasseva. Oxides and nitrides as alternative plasmonic materials in the optical range. *Opt. Mater. Express* **1** (6), 1090 (2011) [DOI: 10.1364/OME.1.001090].
6. W. Allen, M.S. Allen, D.C. Look, B.R. Wenner, N. Itagaki, K. Matsushima, I. Surhariadi. Infrared plasmonics via ZnO. *J. Nano Res.* **28**, 109 (2014) [DOI: 10.4028/www.scientific.net/JNanoR.28.109].
7. M.A. Bodea, G. Sbarcea, G.V. Naik, A. Boltasseva, T.A. Klar, J.D. Pedarnig. Negative permittivity of ZnO thin films prepared from aluminum and gallium doped ceramics via pulsed-laser deposition. *Appl. Phys. A* **110**, 929 (2013) [DOI: 10.1007/s00339-012-7198-6].
8. D.C. Look, K.D. Leedy. ZnO plasmonics for telecommunications. *Appl. Phys. Lett.* **102**, 182107 (2013) [DOI: 10.1063/1.4804984].
9. T.V. Semikina. Atomic layer deposition as a nanotechnological method for functional materials. Review. *Sci. Notes Taurida Nat. Univ. Ser. Phys.* **22** (61), No. 1, 116 (2009) (in Russian).
10. A. Wójcik, M. Godlewski, E. Guzievicz, R. Minikaev, W. Paszkowicz. Controlling of preferential growth mode of ZnO thin films grown by atomic layer deposition. *J. Cryst. Growth* **310**, 284 (2008) [DOI: 10.1016/j.jcrysgro.2007.10.010].
11. T. Krajewski, E. Guzievicz, M. Godlewski, L. Wachicki, I.A. Kowalik, A. Wojcik-Głodowska, M. Lukasiewicz, K. Kopalko, V. Osinniy, M. Guziewicz. The influence of growth temperature and precursors' doses on electrical parameters of ZnO thin films grown by atomic layer deposition technique. *Microelectr. J.* **40**, 293 (2009) [DOI: 10.1016/j.mejo.2008.07.053].
12. E. Przeździecka, Ł. Wachnicki, W. Paszkowicz, E. Łusakowska, T. Krajewski, G. Łuka, E. Guziewicz, M. Godlewski. Photoluminescence, electrical and structural properties of ZnO films, grown by ALD at low temperature. *Semicond. Sci. Technol.* **24**, 105014 (2009) [DOI: 10.1088/0268-1242/24/10/105014].
13. E.F. Venger, O.V. Melnichuk, Yu.A. Pasichnyk. *Spectroscopy of Residual Rays* (Naukova Dumka, 2001) (in Ukrainian).
14. E.F. Venger, A.V. Melnichuk, L.Ju. Melnichuk, Ju.A. Pasechnik. Anisotropy of the ZnO single crystal reflectivity in the region of residual rays. *Phys. Status Solidi (b)* **188** (2), 823 (1995) [DOI: 10.1002/pssb.2221880226].
15. I.P. Kuzmina, V.A. Nikitenko. *Zinc Oxide. Preparation and Optical Properties* (Nauka, 1984) (in Russian).
16. H. Ham, G. Shen, J.H. Cho, T.J. Lee, S.H. Seo, Ch.J. Lee. Vertically aligned ZnO nanowires produced by a catalyst-free thermal evaporation method and their field emission properties. *Chem. Phys. Lett.* **404**, 69 (2005) [DOI: 10.1016/j.cplett.2005.01.084].
17. E.A. Vinogradov, I.A. Dorofeev. *Thermally Induced Electromagnetic Fields of Solids* (Fizmatlit, 2010) (in Russian).
18. E.F. Venger, L.Yu. Melnichuk, O.V. Melnichuk, T.V. Semikina, Yu.I. Khrokolova. IR-reflection spectroscopic study of thin ZnO films on the SiO<sub>2</sub> surface. In *Physico-Mathematical Notes: Collection of Scientific Works* (Nizhyn State Univ., 2013), p. 59 (in Ukrainian).
19. E.F. Venger, D.V. Korbutyak, L.Yu. Melnichuk, O.V. Melnichuk. Research of films of ZnO on the substrate with optical of few down the method IR-spectroscopy of reflection. *Trans. Iakob Gogebashvili Telavi State Univ.* **1** (27), 64 (2014).
20. E.F. Venger, A.V. Melnichuk, Yu.A. Pasechnik, E.I. Sukhenko. Surface polaritons in the system ZnO on sapphire. *Optoelektron. Poluprovodn. Tekhn.* **31**, 120 (1996) (in Russian).

Received 02.12.2015.

Translated from Ukrainian by O.I. Voitenko

Є.Ф. Венгер, Л.Ю. Мельничук,  
О.В. Мельничук, Т.В. Семікіна

#### ДОСЛІДЖЕННЯ МЕТОДАМИ ІЧ-СПЕКТРОСКОПІЇ ТОНКИХ ПЛІВОК ОКСИДУ ЦИНКУ, ВИРОЩЕНИХ МЕТОДОМ АПО

#### Резюме

Уперше методами ІЧ-відбивання та модифікованим методом порушеного повного внутрішнього відбивання (ППВВ) теоретично та експериментально досліджено прозорі провідні нелеговані плівки ZnO, вирощені методом атомного шарового осадження (АПО) в області частот 400–1400 см<sup>-1</sup>. Отримані із спектрів ІЧ-відбивання параметри плівки ZnO вказують на наявність у спектрах ППВВ частотних “вікон”, в яких збуджуються поверхневі фононні та плазмон-фононні поляритони. Теоретичні розрахунки задовільно узгоджуються з експериментальними результатами. Побудовано та досліджено дисперсійні залежності високота низькочастотної гілок спектрів ППВВ.